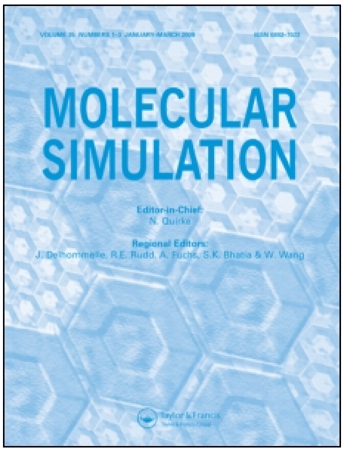

**Molecular Simulation**
Publication details, including instructions for authors and subscription information:
http://www.informaworld.com/smpp/title~content=t713644482

# Another look at organic/metal (O/M) interfaces: correlation with experiment

P. M. Mitrasinovic[a]
[a] Department of Information Technologies and Artificial Intelligence, Institute for Multidisciplinary Research, University of Belgrade, Belgrade, Yugoslavia

**To cite this Article** Mitrasinovic, P. M.(2008) 'Another look at organic/metal (O/M) interfaces: correlation with experiment', Molecular Simulation, 34: 1, 89 — 95
**To link to this Article: DOI:** 10.1080/08927020701730369
**URL:** http://dx.doi.org/10.1080/08927020701730369

*Molecular Simulation*
Vol. 34, No. 1, January 2008, 89–95

# Another look at organic/metal (O/M) interfaces: correlation with experiment

P.M. Mitrasinovic*

*Department of Information Technologies and Artificial Intelligence, Institute for Multidisciplinary Research, University of Belgrade, Kneza Viseslava 1a, 11030 Belgrade, Yugoslavia*

*(Received 5 July 2007; final version received 6 October 2007)*

Topological features of the electron density ($\rho$) at a bond critical point (BCP), determined by the quantum theory of atoms in molecules (QTAIM), were previously established as a determinative factor underlying the nature of an O/M-bonded interaction (P. M. Mitrasinovic, *Can. J. Chem.*, **81**:542–554, 2003). Herein, a general methodology for the extrapolation of the nature of the interfacial interactions is proposed by investigating the changes of organic/metal BCP parameters as consequences of both increasing the size and changing the shape of the metal surfaces. In particular, the adsorption of acrylonitrile (AN) on the model copper (Cu) clusters ($\mathrm{Cu}_n$, $n = 9–14$, 16, 18, 20) simulating the actual Cu(100) surface is analyzed. The electron density and its Laplacian ($\nabla^2$) at the AN/$\mathrm{Cu}_n$ BCPs are statistically correlated with experimental quantities, such as electron affinities (EAs) and ionization potentials (IPs) of metal surfaces. The dipole moment (DM), a chemical descriptor arising directly from the electron density distribution in both the overall (AN/$\mathrm{Cu}_n$) model systems and the $\mathrm{Cu}_n$ clusters, is found to be better-correlated with the experimentally determined EAs of the $\mathrm{Cu}_n$ clusters than with calculated ones.

**Keywords:** organic/metal interfaces; quantum theory of atoms in molecules; electron density distribution; correlation with experiment

## 1. Introduction

In our previous study [1] the quantum theory of atoms in molecules [2] has been fundamentally established as a valuable means of investigating the nature of the interactions between organic molecules (adsorbates) and metallic surfaces. Advantages of the use of finite models for metal surfaces have been shown to be associated with both generating the adsorbate geometry reliably and having the limited size of an entire molecular system involved in quantum-chemical computations at a sophisticated level of theory [1]. There have been theoretical [3,4] and experimental [5–7] confirmations that the size of transition metal clusters substantially influences the chemisorption of an adsorbate. The cluster approach is physically justified as long as chemisorption is treated as a local phenomenon and long-range interactions are neglected [8]. In this context, a general methodology for the extrapolation of the nature of the acrylonitrile/copper (AN/Cu) (100) surface interaction has been proposed using the AN/$\mathrm{Cu}_n$ ($n = 9–14$, 16, 18, 20) bond critical point parameters [9]. The key beauty of this novel strategy is that the definition of a bonded interaction becomes free of any assumptions, fully physical and convenient to be visualized by means of the topological features of the total electron density [1,9]. In this paper, the electron distribution in the AN/$\mathrm{Cu}_n$ complexes dissected through the electron density and Laplacian at the AN/$\mathrm{Cu}_n$ BCPs is statistically correlated with measurable variables, such as the electron affinities and ionization potentials of the $\mathrm{Cu}_n$ clusters.

## 2. Methodology

The adsorption of AN on the (100) surface of the fcc copper crystal is simulated by use of several copper clusters having the sizes between 9 and 20 atoms, as shown schematically in Figure 1. The clusters have two layers of atoms and are denoted by $\mathrm{Cu}_n(k, l)$. The subscript $n$ denotes the total number of copper atoms in the cluster. The numbers $k$ and $l$ ($k + l = n$) within parentheses indicate the number of copper atoms located in the upper and bottom layers, respectively. The adsorption of AN on $\mathrm{Cu}_9(5, 4)$ was shown to include two copper atoms, of which the first is the central atom (Cu1 in Figure 1) and the second is an edge atom (Cu2 in Figure 1) of the cluster [8]. The central atom of the upper layer has the same number of nearest neighbors as an actual surface atom, while the edge atom is unsaturated with reference to one on the actual (100) surface. Hence, the $\mathrm{Cu}_9(5, 4)$ cluster has been enlarged to saturate the peripheral binding site by extending both the upper layer

---

*Email: petar.mitrasinovic@cms.bg.ac.yu

ISSN 0892-7022 print/ISSN 1029-0435 online

DOI: 10.1080/08927020701730369
http://www.informaworld.com

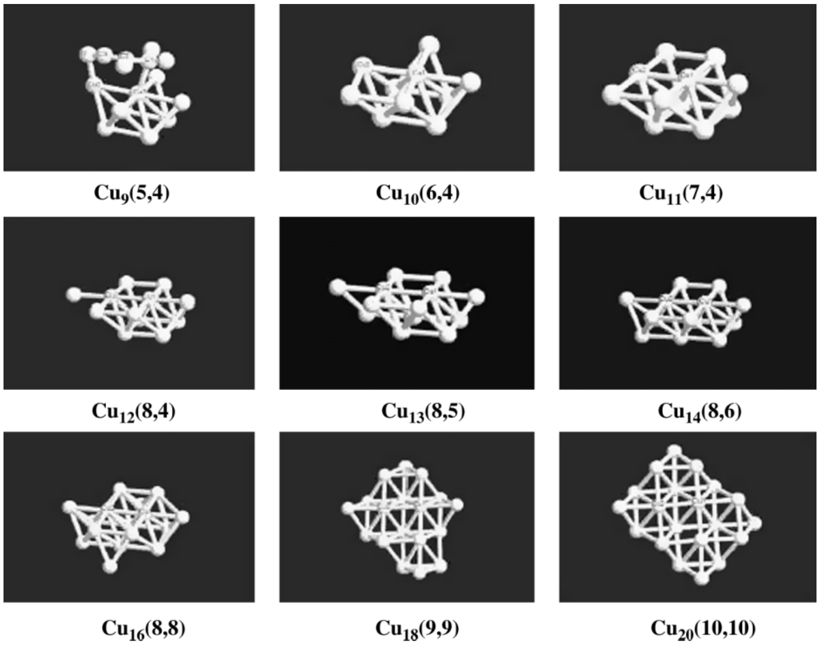

Figure 1. Clusters $Cu_n(k, l)$ simulating the Cu (100) surface. $n$-total number of atoms in clusters, $k$-number of atoms in the upper layer, $l$-number of atoms in the bottom layer. AN is bonded to Cu1 and Cu2 in all the complexes. Since Cu1 has the same number of nearest neighbors as an actual surface atom, we focus on the interfacial interactions between C1 in AN and Cu1 in $Cu_n(k, l)$.

in $Cu_{10}(6, 4)$, $Cu_{11}(7, 4)$ and $Cu_{12}(8, 4)$ and the bottom layer in $Cu_{13}(8, 5)$ and $Cu_{14}(8, 6)$. The $Cu_{14}(8, 6)$ cluster has two central atoms with the same number of nearest neighbors as on the actual (100) surface. Denote the two central atoms by Cu1 and Cu2 in Figure 1. $Cu_{16}(8, 8)$, $Cu_{18}(9, 9)$ and $Cu_{20}(10, 10)$ have the same two central atoms too. AN was placed above the two central copper atoms before optimizing the complexes. There are indications that the copper atoms with the lowest spin density represent the most likely interaction sites [8]. In all the clusters, the concentration of the spin density is most pronounced in the vicinity of the peripheral Cu atoms of the upper layer. The unsaturated edge atoms having the lowest coordination number are not expected to simulate the copper surface (100) atoms as reliably as the central atoms of the upper layer. Thus, the interfacial interaction between C1 in AN and Cu1 in $Cu_n(k, l)$ is looked upon as being more physically realistic. Values of the electron density and Laplacian at the AN/$Cu_n$ BCPs are those obtained by density functional theory (DFT) calculations, as elucidated in Refs. [1,9]. The specific level of theory and the basis set employed are given in the title of Table 1. The experimental EAs of the $Cu_n$ clusters taken from the literature [8] are: 2.40 eV for $Cu_9$, 2.05 eV for $Cu_{10}$, 2.42 eV for $Cu_{11}$, 2.10 eV for $Cu_{12}$, 2.30 eV for $Cu_{13}$, 2.00 eV for $Cu_{14}$, 2.55 eV for $Cu_{16}$, 2.60 eV for $Cu_{18}$ and 1.97 eV for $Cu_{20}$. The cluster size-dependent approximations used for calculating the EAs and IPs of the $Cu_n$ clusters are: $EA(n) = 4.65 - 5.073 \times n^{-1/3}$ and $IP(n) = 4.65 + 3.166 \times n^{-1/3}$, [8]. The $\rho$, $\nabla^2$ and dipole moment DM vs. EA and IP data sets were fitted by using the "least squares" method.

## 3. Results

The nature of the AN/Cu (100) surface interfacial interaction is determined by extrapolating the AN/$Cu_n$ ($n = 9-14, 16, 18, 20$) bond-critical parameters from a statistical standpoint. The AN/$Cu_n$ bond-critical parameters are given in Table 1. The interatomic distances $d$

Table 1. The B3LYP/6-31+G* electron density and its Laplacian at the C1—Cu1 BCPs† followed by the DMs, EAs and IPs of the $Cu_n$ clusters in AN/$Cu_n$.

| *Complex* | $\rho$ | $\nabla^2$ | *DM*‡ | *DM*¶ | *EA*§ | *EA*‖ | *IP*# |
|---|---|---|---|---|---|---|---|
| AN/$Cu_9$ | 0.56 | 2.14 | 18.66 | 3.65 | 2.40 | 2.13 | 6.12 |
| AN/$Cu_{10}$ | 0.53 | 2.31 | 21.65 | 7.04 | 2.05 | 2.34 | 6.22 |
| AN/$Cu_{11}$ | 0.48 | 2.21 | 22.67 | 7.79 | 2.42 | 2.44 | 6.29 |
| AN/$Cu_{12}$ | 0.51 | 2.33 | 35.87 | 31.89 | 2.10 | 2.48 | 6.31 |
| AN/$Cu_{13}$ | 0.49 | 2.20 | 31.25 | 27.01 | 2.30 | 2.33 | 5.90 |
| AN/$Cu_{14}$ | 0.52 | 2.22 | 25.76 | 4.92 | 2.00 | 2.52 | 5.77 |
| AN/$Cu_{16}$ | 0.49 | 2.16 | 23.22 | 4.21 | 2.55 | 2.66 | 5.66 |
| AN/$Cu_{18}$ | 0.47 | 1.97 | 29.44 | 5.91 | 2.60 | 2.69 | 5.82 |
| AN/$Cu_{20}$ | 0.55 | 2.09 | 26.33 | 5.11 | 1.97 | 2.91 | 5.79 |

† BCP = the C1—Cu1 bond-critical point, $\rho = \rho(BCP)$ in e/Å$^3$, $\nabla^2 = \nabla^2\rho(BCP)$ in e/Å$^5$. ‡ Calculated DMs of the AN/$Cu_n$ complexes in debye. ¶ Calculated DMs of the $Cu_n$ clusters in the AN/$Cu_n$ complexes. § Experimental EAs of the $Cu_n$ clusters in eV. ‖ Calculated EAs of the $Cu_n$ clusters in eV. # Calculated IPs of the $Cu_n$ clusters in eV.

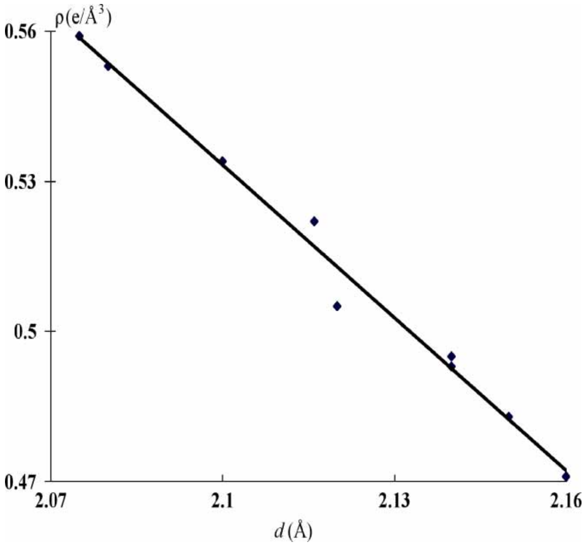

Figure 2. Correlation of $d$ and $\rho$ (Equation (1)).

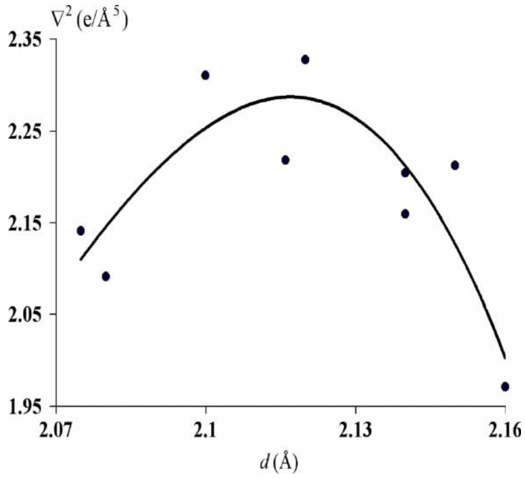

Figure 3. Correlation of $d$ and $\nabla^2$ (Equation (5)).

in this paper are given in Å, the electron density $\rho = \rho$BCP is in e/Å$^3$, the Laplacian $\nabla^2 = \nabla^2\rho$BCP is in e/Å$^5$ and the DMs in debye (D). The standard deviations $\sigma_f$ of a fit (for $f$ degrees of freedom) are quoted as a percent of the observed range of the dependent variable, for example, $\sigma_9 = 0.0033 \sim 3.7\%$. The observed ranges of $\rho$, $\nabla^2$ and DMs are 0.088 e/Å$^3$, 0.36 e/Å$^5$, 17.21 and 28.24 debye, respectively (Table 1).

$\rho$ increases monotonically with decreasing $d$ in Figure 2. This dependence can be represented by a linear, or a logarithmic, or a power, or an exponential function. The observed range of $\rho$ is 0.088. A linear regression yields

$$\rho = -1.017d + 2.669 \tag{1}$$

($r^2 = 0.987$, $\sigma_7 = 0.0033 \sim 3.7\%$), a logarithmic regression yields

$$\rho = -2.152\ln(d) + 2.129 \tag{2}$$

($r^2 = 0.987$, $\sigma_7 = 0.0033 \sim 3.7\%$), a power regression yields

$$\rho = 11.753d^{-4.171} \tag{3}$$

($r^2 = 0.986$, $\sigma_7 = 0.0034 \sim 3.8\%$) and an exponential regression yields

$$\rho = 33.449\exp(-1.971d) \tag{4}$$

($r^2 = 0.986$, $\sigma_7 = 0.0034 \sim 3.8\%$). All the correlations are quite satisfactory with respect to the observed range of the dependent variable. As all values of the electron density at the BCPs hover around 0.5 that is typically associated with weak donor–acceptor bonds [10,11], a value of the $d$ coordinate of 2.624 at which $\rho$, approximated by Equation (1) is equal to 0 has no a particular physical meaning.

The variation of $\nabla^2$ with $d$ is approximated by a cubic polynomial (Figure 3)

$$\nabla^2 = -629.15d^3 + 3869.2d^2 - 7923.2d + 5404 \tag{5}$$

($r^2 = 0.739$, $\sigma_5 = 0.0668 \sim 18.7\%$). The regression line has a maximum of 2.29 at $d = 2.12$ and crosses the $\nabla^2 = 0$ line at $d = 2.05$ and $d = 2.17$. The $\nabla^2$ vs. $\rho$ plot is of the type observed for the correlation of $d$ and $\nabla^2$. A cubic correlation over the entire $\rho$, $\nabla^2$ data range is

$$\nabla^2 = 818.73\rho^3 - 1385.3\rho^2 + 775.26\rho - 141.38 \tag{6}$$

($r^2 = 0.735$, $\sigma_5 = 0.0538 \sim 15.1\%$), with a $\nabla^2$ maximum of 2.28 at $\rho = 0.515$ and $\nabla^2 = 0$ at $\rho = 0.468$ and $\rho = 0.587$.

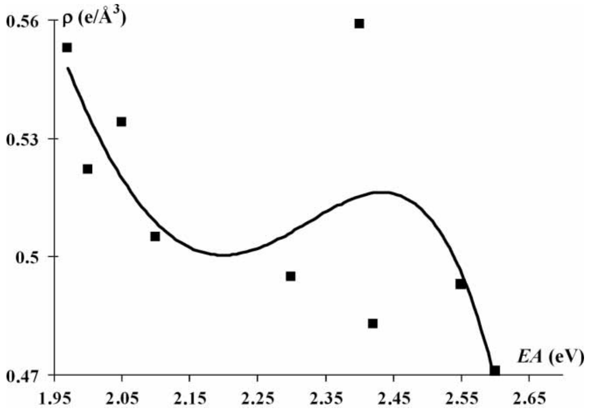

Figure 4. Correlation of experimental EA and $\rho$ (Equation (7)).

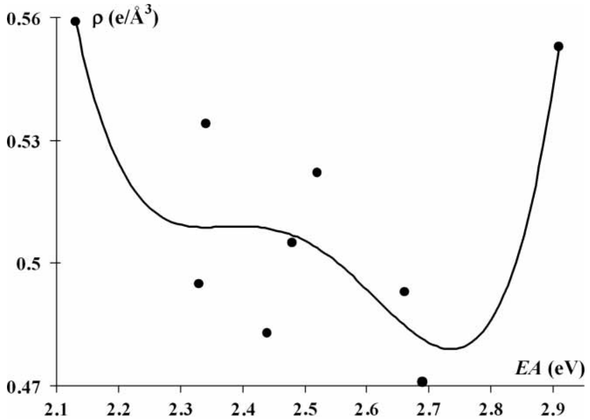

Figure 5. Correlation of calculated EA and $\rho$ (Equation (8)).

The correlation of experimental EA and $\rho$ (Figure 4) is

$$\rho = -2.54\,\mathrm{EA}^4 + 21.03\,\mathrm{EA}^3 - 64.31\,\mathrm{EA}^2 + 85.80\,\mathrm{EA} - 41.41 \qquad (7)$$

($r^2 = 0.534$, $\sigma_4 = 0.0201 \sim 22.7\%$).

The correlation of calculated EA and $\rho$ (Figure 5) is

$$\rho = 5.22\,\mathrm{EA}^4 - 52.01\,\mathrm{EA}^3 + 193.93\,\mathrm{EA}^2 - 320.72\,\mathrm{EA} + 199 \qquad (8)$$

($r^2 = 0.741$, $\sigma_4 = 0.0150 \sim 17.1\%$).

The correlation of calculated IP and $\rho$ (Figure 6) is

$$\rho = 105.39\,\mathrm{IP}^5 - 3164\,\mathrm{IP}^4 + 37981\,\mathrm{IP}^3 - 227861\,\mathrm{IP}^2 + 683217\,\mathrm{IP} - 819064 \qquad (9)$$

($r^2 = 0.662$, $\sigma_3 = 0.0307 \sim 35.2\%$).

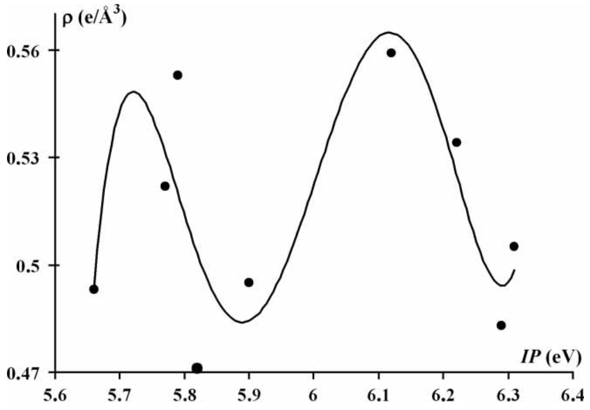

Figure 6. Correlation of calculated IP and $\rho$ (Equation (9)).

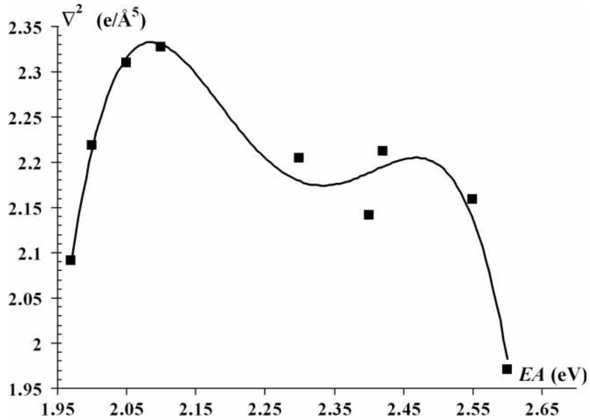

Figure 7. Correlation of experimental EA and $\nabla^2$ (Equation (10)).

The correlation of experimental EA and $\nabla^2$ (Figure 7) is

$$\nabla^2 = -60.39\,\mathrm{EA}^4 + 554.50\,\mathrm{EA}^3 - 1904.91\,\mathrm{EA}^2 + 2901\,\mathrm{EA} - 1650.21 \qquad (10)$$

($r^2 = 0.960$, $\sigma_4 = 0.2465 \sim 67.4\%$).

The correlation of calculated EA and $\nabla^2$ (Figure 8) is

$$\nabla^2 = 20.85\,\mathrm{EA}^4 - 205.58\,\mathrm{EA}^3 + 755.66\,\mathrm{EA}^2 - 1227.5\,\mathrm{EA} + 745.84 \qquad (11)$$

($r^2 = 0.740$, $\sigma_4 = 0.0539 \sim 15.1\%$).

The correlation of calculated IP and $\nabla^2$ (Figure 9) is

$$\nabla^2 = 0.48\,\mathrm{IP}^4 - 12.70\,\mathrm{IP}^3 - 126.39\,\mathrm{IP}^2 - 556.64\,\mathrm{IP} + 917.19 \qquad (12)$$

($r^2 = 0.463$, $\sigma_4 = 0.0979 \sim 21.5\%$).

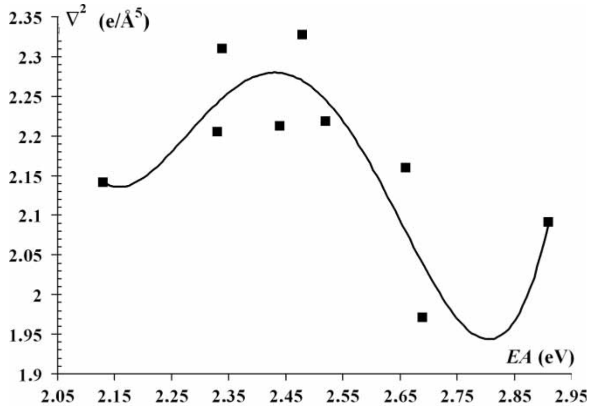

Figure 8. Correlation of calculated EA and $\nabla^2$ (Equation (11)).

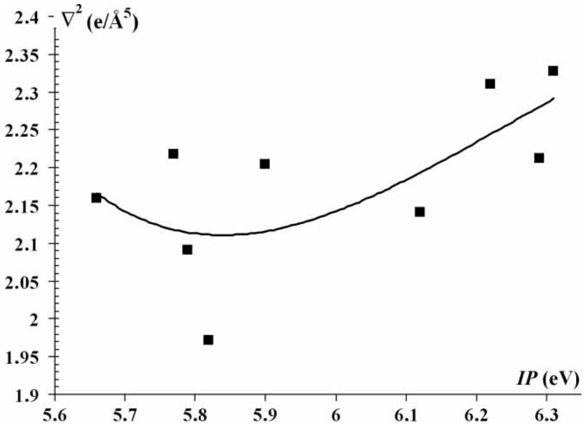

Figure 9. Correlation of calculated IP and $\nabla^2$ (Equation (12)).

The correlation of experimental EA and the DM of $Cu_n$ clusters (Figure 10) is

$$\mathrm{DM} = 1005.2\,\mathrm{EA}^3 - 7084.2\,\mathrm{EA}^2 + 16541\,\mathrm{EA} - 12779 \qquad (13)$$

($r^2 = 0.647$, $\sigma_5 = 8.67 \sim 30.7\%$).

The correlation of calculated EA and the DM of $Cu_n$ clusters (Figure 11) is

$$\mathrm{DM} = 321.92\mathrm{EA}^3 - 2489.1\mathrm{EA}^2 + 6365\mathrm{EA} - 5372 \qquad (14)$$

($r^2 = 0.306$, $\sigma_5 = 11.28 \sim 39.9\%$).

The correlation of experimental EA and the DM of AN/$Cu_n$ (Figure 12) is

$$\mathrm{DM} = 537.5\,\mathrm{EA}^3 - 3702.6\,\mathrm{EA}^2 + 8457.8\,\mathrm{EA} - 6378.4 \qquad (15)$$

($r^2 = 0.393$, $\sigma_5 = 5.1668 \sim 32.9\%$).

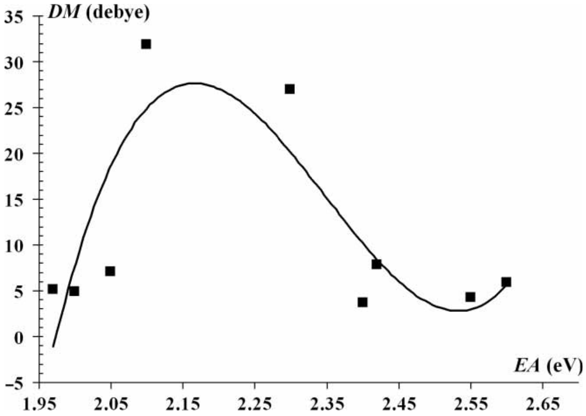

Figure 10. Correlation of experimental EA and DM of $Cu_n$ clusters (Equation (13)).

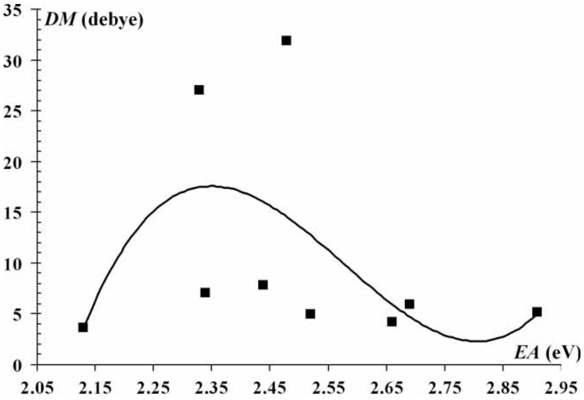

Figure 11. Correlation of calculated EA and DM of $Cu_n$ clusters (Equation (14)).

The correlation of calculated EA and the DM of AN/$Cu_n$ (Figure 13) is

$$\mathrm{DM} = 82.53\,\mathrm{EA}^3 - 658.36\,\mathrm{EA}^2 + 1743.1\,\mathrm{EA} - 1504.9 \qquad (16)$$

($r^2 = 0.284$, $\sigma_5 = 5.72 \sim 33.2\%$).

The “calculated EA vs. experimental EA” plot (Figure 14) is defined by

$$\mathrm{EA}_{\mathrm{calc}} = -5.41\,\mathrm{EA}_{\mathrm{exp}}^3 + 42.37\,\mathrm{EA}_{\mathrm{exp}}^2 - 108.38\,\mathrm{EA}_{\mathrm{exp}} + 93.25 \qquad (17)$$

($r^2 = 0.693$, $\sigma_5 = 0.1811 \sim 22.8\%$).

## 4. Summary

As long as a cluster approach for the simulation of actual Cu (100) surface is physically justified, the nature of an AN/$Cu_n$ interfacial interaction, determined by the

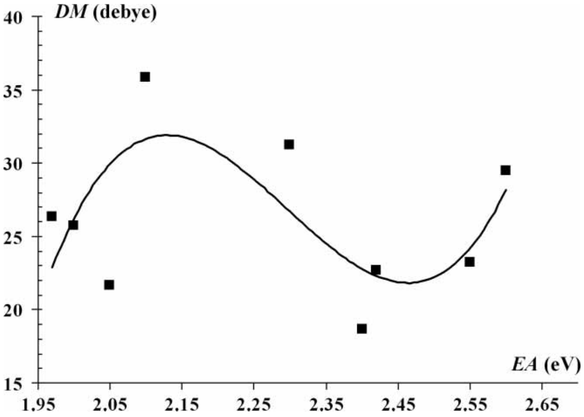

Figure 12. Correlation of experimental EA and DM of AN/$Cu_n$ complexes (Equation (15)).

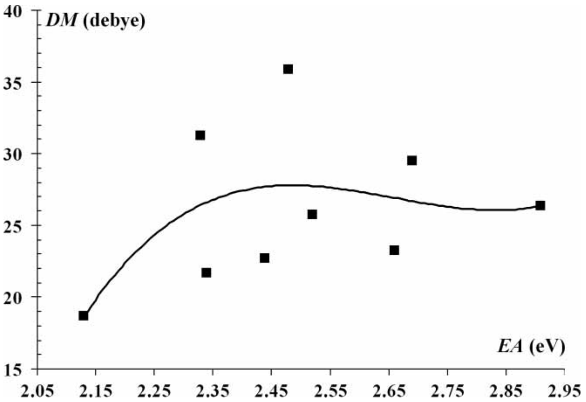

Figure 13. Correlation of calculated EA and DM of AN/$Cu_n$ complexes (Equation (16)).

electron density and its Laplacian at the AN/$Cu_n$ ($n = 9$–14, 16, 18, 20) BCPs, is herein correlated with the electronic properties and reactivity of various copper clusters, dissected through experimentally measurable variables such as the EAs and IPs of $Cu_n$. The statistical models reported in this study define the polynomial correlations being of the third and fourth order mainly. The electron density is found to be substantially better correlated with calculated electronic affinities (Equation (8)) than with experimental ones (Equation (7)). In contrast, the Laplacian is found to be perfectly correlated with experimental electronic affinities (Equation (10)) showing a much higher cross-correlation coefficient than that based on calculated EAs (Equation (11)). Besides, the electron density is found to be much better correlated (Equation (9)) than the Laplacian (Equation (12)) with calculated IPs.

The difference between the electron density and its Laplacian can be rationalized by considering the QTAIM [2]. According to this theory, the specific AN/$Cu_n$-bonded interactions between C1 and Cu1 (Figure 1) are defined by the C1—Cu1 bond paths, which are the lines of the highest electron density linking the bonded pair of atoms. The point of a line of the highest electron density where the gradient, $\nabla\rho(r)$, of the density $\rho(r)$ is equal to zero, is the BCP. The properties of the density at this point give the characteristics of a bond. In contrast, the Laplacian of the electron density ($\nabla^2\rho(r)$) indicates where the electron density is locally concentrated ($\nabla^2\rho(r) < 0$) and depleted ($\nabla^2\rho(r) > 0$) and therefore, contains a large amount of chemical information. Thus, the DM, a chemical descriptor arising directly from the electron density distribution, can be viewed as a reminiscent of the Laplacian. In this context, the DM in both the $Cu_n$ clusters and the overall AN/$Cu_n$ complexes is found to be better-correlated with the experimentally determined EAs of the $Cu_n$ clusters (Equations (13) and (15)) than with calculated ones (Equations (14) and (16)).

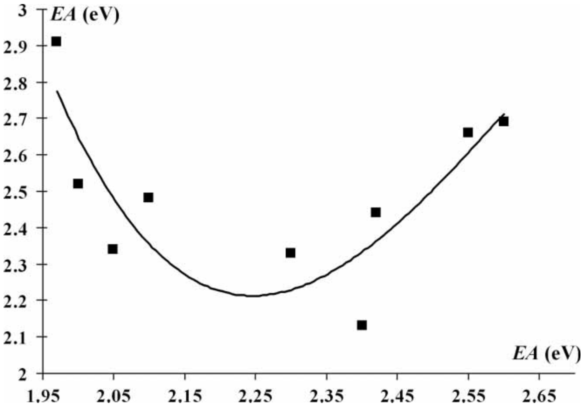

Figure 14. Correlation of measured EA and calculated EA of $Cu_n$ clusters (Equation (17)).

This work supplements our previous studies [1,9] in which the QTAIM was fundamentally established as a valuable means of investigating the nature of the interactions between organic molecules and metallic surfaces from the invariant standpoints. The key beauty of this novel strategy essentially associated with the electronic properties and reactivity of various $Cu_n$ clusters is that no reference to non-invariant concepts, such as orbitals, has been invoked. As the proposed methodology is independent of the scale and size of particular molecular components, its potential applications in changing and tuning the finest details of charge transfer taking place at the donor–acceptor interfaces is quite certain.

## Acknowledgements

This work has been done within the framework of the Project No. 143016B financed by the Ministry of Science of the Republic of Serbia.

## References

[1] P.M. Mitrasinovic, *Acrylonitrile (AN)–$Cu_9$(100) interfaces: electron distribution and nature of bonded interactions*, Can. J. Chem. 81 (2003), p. 542.

[2] R.F. W. Bader, *Atoms in Molecules*, Clarendon Press, Oxford, 1990.

[3] I. Panas, J. Schule, P. Siegbahn, and U. Wahlgren, *On the cluster convergence of chemisorption energies*, Chem. Phys. Lett. 149 (1988), p. 265.

[4] V. Russier, D.R. Salahub, and C. Mijoule, *Theoretical determination of work functions and adsorption energies of atoms on metal surfaces from small-cluster calculations: a local-spin-density approach*, Phys. Rev. B 42 (1990), p. 5046.

[5] M.D. Morse, M.E. Geusic, J.R. Heat, and R.E. Smalley, *Surface reactions of metal clusters II. Reactivity surveys with $D_2$, $N_2$ and CO*, J. Chem. Phys. 83 (1985), p. 2293.

[6] R.L. Whetten, D.M. Cox, D.J. Trevor, and A. Caldor, *Correspondence between electron binding energy and chemisorption reactivity of iron clusters*, Phys. Rev. Lett. 54 (1985), p. 1494.

[7] J.S. Bradley, J.M. Millar, E.W. Hill, S. Behal, B. Chaudret, and A. Duteil, *Surface chemistry on colloidal metals—spectroscopic study of adsorption of small molecules*, Faraday Discuss. 92 (1991), p. 255.

[8] X. Crispin, C. Bureau, V. Geskin, R. Lazzaroni, and J.L. Bredas, *Local density functional study of copper clusters: a comparison between real clusters, model surface clusters, and the actual metal surface*, Eur. J. Inorg. Chem. (1999), p. 349.

[9] P.M. Mitrasinovic, *Another look at organic/metal interfaces: correlation with experiment*, paper presented at the NSTI Nanotech 2007 Conference, Santa Clara, CA, 20–24 May 2007.

[10] P.M. Mitrasinovic, *Invariant description of the behavior of electrons in donor–acceptor molecules*, Chem. Phys. Lett. 392 (2004), p. 419.

[11] P.M. Mitrasinovic, *Electron delocalization in atomic and molecular systems*, J. Phys. Chem. A 106 (2002), p. 11262.